TIMING, ABUNDANCE, AND SPATIAL EXTENT OF INITIAL MAGMATISM ON THE MOON EXPLAINED BY CUMULATE MANTLE OVERTURN. T. C. Prissel[1], N. Zhang[2,3], C. R. M. Jackson[4], H. Li[5]. [1]NASA Johnson Space Center, Houston, TX, USA (tabb.c.prissel@nasa.gov). [2]Peking University, Beijing, China (nan_zhang@pku.edu.cn). [3]Curtin University, Bentley, Perth, Western Australia. [4]Tulane University, New Orleans, LA, USA. [5]University of California, Davis, CA, USA.

Preface: We have recently quantified the timing, abundance, and spatial extent of lower mantle melting induced by cumulate overturn on the Moon through a series of 3D geodynamical models [1]. Our dynamical modeling indicates that overturn of thin (~30-50 km) and weak [2] ilmenite-bearing cumulates (IBC) triggers a rapid, short-lived, and widespread period of lower mantle melting which reproduces the key geochronological, volume, and spatial characteristics associated with the onset of secondary magmatism on the Moon (Figs. 1,2), and without energy contributions from KREEP (potassium, rare earth elements, phosphorus, radiogenic U, Th). Within the guiding paradigms of global differentiation via magma ocean crystallization and subsequent cumulate mantle overturn, our model provides explanation for near contemporaneous primary and secondary crust production constrained by geochronology of returned lunar samples and meteorites [3-5].

In this abstract, we discuss our results in context with several intricacies of lunar chronology including models of a long-lived magma ocean [6-8], the hypothesis that mantle overturn was induced by the giant South Pole-Aitken basin forming impact [9,10], and ancient lunar zircon [11-13].

Mantle Overturn During a Long-lived Residual Magma Ocean: Lunar magma ocean (LMO) solidification is likely rapid for the first 80% of crystallization [6], whereas the final ~20% can be prolonged up to ~200 Myrs due to an insulating ferroan anorthositic crust (FAN) [7,8]. An extended duration of residual magma ocean solidification could exceed the time to initiate overturn of the silicate mantle itself [6], resulting in syn-FAN decompression melting of the lower mantle. In this way, silicate-driven overturn generally works toward reconciling a contemporaneous relationship between primary FAN and the onset of secondary magmatism (Mg-suite) while also allowing

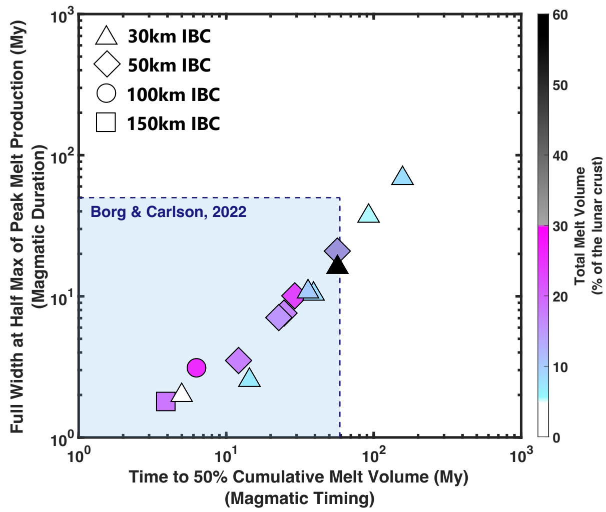

Fig. 1. From Prissel et al., (2023). Duration and timing of magmatism induced by cumulate overturn with color scale correlated to total melt volume (reported in vol. % of the total lunar crust). Geochronological constraints defined by blue-shaded region [4] indicate a relatively short magmatic duration and rapid magmatic timing for Mg-suite petrogenesis. Model data shows that magmatic timing and magmatic duration are positively correlated phenomena during cumulate mantle overturn. Results indicate that partial melting of the KREEP-poor lower mantle during cumulate overturn can simultaneously satisfy the onset, duration, and abundance constraints (~6-30 vol.% of the total lunar crust) of Mg-suite magmatism.

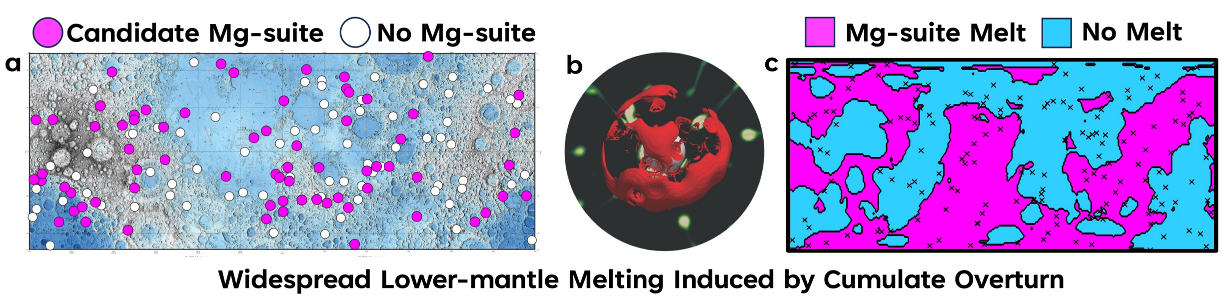

Fig. 2. Figures modified from Prissel et al., (2023). **a)** Global extent of candidate Mg-suite exposures across the lunar surface [14]. **b)** Snapshot of a dynamical overturn model near peak melt production and highlighting the 3D melt surface of the widespread upwelling KREEP-poor lower mantle (red). The 3D melt surface overlays an isolated 2D slice of the downwelling IBC (yellow-green to gray) relative to all other interior components (black). **c)** 2D global surface expression for regions of lower-mantle melting (pink) and no melting (blue) from the dynamical model shown in b).

for an extended formation interval of primary crust production. Still, petrologic and geochronologic context requires that FAN formation preceded secondary magmatic intrusions or ancient volcanic eruptions.

Here it is important to note that LMO models [6,15-17] consistently predict formation of the high-density IBC layer after FAN production and prior to both urKREEP formation and complete LMO solidification, i.e., during the timeframe allotted to the hypothesized long-lived residual magma ocean [1]. This is critical to future models because the formation of IBC reduces overturn initiation timescales to thousands of years [6]. For instance, our results of IBC-driven overturn [1] remain valid considering long-lived residual magma oceans since the time zero of our model is predicated on the isotopic closure ages of primary FAN and not the complete solidification age of the LMO itself. Within the evidence-based framework indicating a petrogenetic link between mantle overturn and Mg-suite, our results thus imply that the formation of an IBC layer during LMO differentiation occurred within millions to tens of millions of years of FAN closure [1].

Implications Concerning the South Pole-Aitken Basin Forming Impact: It is also possible that the South Pole-Aitken (SPA) basin forming impact triggered mantle overturn [18], resulting in both the geochemical asymmetry of the lunar surface [9,10,19] and Mg-suite production. Dynamical models of the SPA impact [8] predict rapidly induced and widespread mantle convection like our modeling shows. If secondary crust building was initiated by SPA, geochronology then requires that FAN closure (~4361 Ma) and the SPA impact be coincident. A minimum age of ~4.3 Ga has been inferred for SPA based on Gravity Recovery and Interior Laboratory data [20], consistent with the hypothesis above. Samples returned from SPA are needed to fully test this hypothesis, however, and our study of early mantle convection [1] further emphasizes the need for sample return beyond SPA such as primary crust or ancient igneous deposits from the lunar farside highlands [21].

Lunar Zircon & Implications: Other studies have leveraged U-Pb and Lu-Hf systematics in both detrital and in situ lunar zircon [11-13]. These studies suggest Moon solidification occurred between 4.51 – 4.46 Ga, and that Mg-suite magmatism itself may have initiated at ~4.46 Ga [11,12] (Fig. 3, Civet Cat norite 72255).

We have demonstrated that magmatic timing and duration are positively correlated phenomena for overturn-induced secondary crust building (Fig. 1). Early or ancient magmatism inferred from 72255 is therefore not expected to also be long-lived based on our modeling. Our results therefore suggest that **i)** mechanisms other than mantle overturn produced

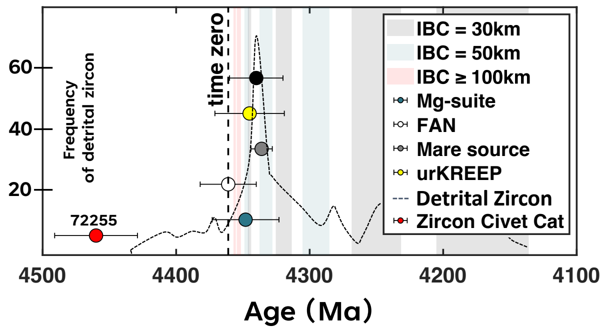

Fig. 3. Adapted from Borg & Carlson (2022) and Prissel et al., (2023), summarizing ages of primary LMO products, secondary magmatism (Mg-suite), detrital zircon, and zircon from Civet Cat norite 72255 [11,12], relative to modeled magmatic timing and duration from Prissel et al., (2023) (time zero of our model signified by vertical dashed line, where the onset and duration of magmatism for each model is defined by vertical colored bars).

ancient zircon-bearing noritic samples or **ii)** an alternative global evolutionary event is responsible for the younger and various igneous products with concordant formation ages of ~4.35 Ga (Fig. 3). Here we note that ancient magmatic duration constraints have not yet been established through study of lunar zircon, meaning this scenario cannot be fully tested in light of our dynamical modeling of mantle overturn. Whereas we show that overturn naturally results in near-contemporaneous primary and secondary crust building, which is entirely consistent with current rheological constraints [2,22] and geochronology of putative primary crust, mantle sources, secondary Mg-suite, and the peak of detrital zircon ages (Fig. 3). Regardless, we maintain that gravitational instabilities in magma ocean cumulate piles are major driving forces for the dynamics of early mantle convection within and initial secondary crust building on differentiated bodies [6,23-25].

References: [1] Prissel, T.C. et al. (2023) *Nat. Comm., 14* [2] Dygert, N. et al. (2016) *GRL 43* [3] Borg, L.E. et al., (2020) *GCA 290* [4] Borg, L.E. & Carlson, R.W. (2022) *Annu. Rev. Earth Planet. Sci. 51* [5] Zhang, B., et al., (2021) *EPSL 569* [6] Elkins-Tanton, L.T. et al., (2011) *EPSL 304* [7] Maurice, M. et al., (2020) *Sci. Adv. 6* [8] Michaut, C. & Neufeld, J.A. (2022) *GRL 49* [9] Zhang, N. et al., (2022) *Nat. Geosci. 15* [10] Jones, M.J. et al., (2022) *Sci. Adv. 8* [11] Zhang, B. et al. (2021) *GCA 302* [12] Greer, J. et al. (2023) *Geochem. Persp. Lett. 27* [13] Barboni, M. et al. (2017) *Sci. Adv. 6* [14] Sun, Y. et al. (2017) *EPSL 465* [15] Lin, Y. et al., (2016) *Nat. Geosci. 10* [16] Rapp, J. & Draper, D. (2018) *MAPS 53* [17] Charlier, B. et al. (2018) *GCA 234* [18] Moriarty, D.P. III et al. (2021) JGR 126 [19] Laneuville, M. et al. (2013) *GRL 118* [20] Evans, A.J. et al. (2018) *JGR 123* [21] Izquierdo, K. et al. (this conference) [22] Li, H. et al. (2019) *JGR 124* [23] Boukaré, C.-E. et al., (2018) *EPSL 491* [24] Mallik, A. et al. (2019) *GCA 250* [25] Mouser, M.D. & Dygert, N. (2023) *JGR 128*